

Effects of Layer Stacking on the Combination Raman Modes in Graphene

Rahul Rao,^{†,*} Ramakrishna Podila,[‡] Ryuichi Tsuchikawa,[§] Jyoti Katoch,[§] Derek Tishler,[§] Apparao M. Rao,[‡] and Masa Ishigami[§]

[†]Materials and Manufacturing Directorate, Air Force Research Laboratory, WPAFB, Ohio 45433, United States, [‡]Department of Physics and Astronomy, Clemson University, Clemson, South Carolina 29634, United States, and [§]Department of Physics and Nanoscience Technology Center, University of Central Florida, Orlando, Florida 32816, United States

Single layer (SLG) and bilayer graphene (BLG) have recently attracted much attention from the research community, mainly due to their extraordinary electronic properties, which are interesting for both fundamental and applied sciences.^{1,2} SLG and BLG are quite different from each other with respect to their band structure. SLG is a semimetal with a vanishing density of states at the Fermi level,³ while AB-stacked BLG possesses massive Dirac fermions with a transverse field-tunable band gap.⁴ On the other hand, incommensurate BLG (IBLG) behaves in a similar fashion as SLG with reduced Fermi velocities.^{5,6}

Raman spectroscopy is the standard technique to distinguish between SLG, BLG, IBLG, and graphene samples with a few layers (FLG).⁷ The most commonly used Raman signature for layer thickness is a peak occurring at $\sim 2700\text{ cm}^{-1}$ called the 2D (also called the G') band, which is an overtone of the disorder-induced D band located at $\sim 1350\text{ cm}^{-1}$. Both the D and 2D bands occur due to an intervalley double resonance Raman process⁸ where the D band phonon scattering is a second order process mediated by a defect, while the 2D band occurs due to scattering by two phonons and does not need any defects for activation. The 2D band in SLG can be fit to a single Lorentzian peak and its intensity has been found to be much higher than that of the G band (located at $\sim 1580\text{ cm}^{-1}$) for SLG; hence it is often used as an indicator of an SLG region.^{7,9–12} On the other hand, the 2D band in BLG can be clearly deconvoluted into four Lorentzian peaks and its intensity is lower than that of the 2D band in SLG on silicon dioxide.⁷ As the number of layers increase to more than 3 the 2D band evolves into a two-peak structure along

ABSTRACT We have observed new combination modes in the range from 1650 to 2300 cm^{-1} in single-(SLG), bi-, few-layer and incommensurate bilayer graphene (IBLG) on silicon dioxide substrates. A peak at $\sim 1860\text{ cm}^{-1}$ (iTA LO^-) is observed due to a combination of the in-plane transverse acoustic (iTA) and the longitudinal optical (LO) phonons. The intensity of this peak decreases with increasing number of layers and this peak is absent for bulk graphite. The overtone of the out-of-plane transverse optical (oTO) phonon at $\sim 1750\text{ cm}^{-1}$, also called the M band, is suppressed for both SLG and IBLG. In addition, two previously unidentified modes at ~ 2200 and $\sim 1880\text{ cm}^{-1}$ are observed in SLG. The 2220 cm^{-1} (1880 cm^{-1}) mode is tentatively assigned to the combination mode of in-plane transverse optical (iTO) and TA phonons (oTO+LO phonons) around the K point in the graphene Brillouin zone. Finally, the peak frequency of the 1880 (2220) cm^{-1} mode is observed to increase (decrease) linearly with increasing graphene layers.

KEYWORDS: graphene · Raman · spectroscopy · double resonance · combination

with a concomitant decrease in intensity with respect to the G band. It has recently been shown that IBLG can be distinguished between SLG and BLG by the presence of a new defect-induced peak (I band) located on the high-frequency side of the D band (Figure 1a).¹³ The I band appears due to one layer imposing a perturbation on the other and is a signature for the presence of non-AB stacked graphene. Moreover, the frequency of the I band depends on the angle of orientation between the folded and parent graphene layer.¹³ In another recent report, other weak intensity peaks between 1650 and 2150 cm^{-1} have been observed from SLG and IBLG.¹⁴ These weak intensity peaks were assigned to combination modes that occur due to a double resonance Raman scattering process involving the in-plane transverse optical (iTO), longitudinal optical (LO), and in-plane transverse acoustic (iTA) phonons.¹⁴

We have performed detailed investigations of the combination modes involving iTO, LO, and iTA phonons in SLG, BLG, FLG, and IBLG and report three new features in

*Address correspondence to rahul.rao@wpafb.af.mil.

Received for review November 15, 2010 and accepted December 24, 2010.

Published online January 04, 2011
10.1021/nn1031017

© 2011 American Chemical Society

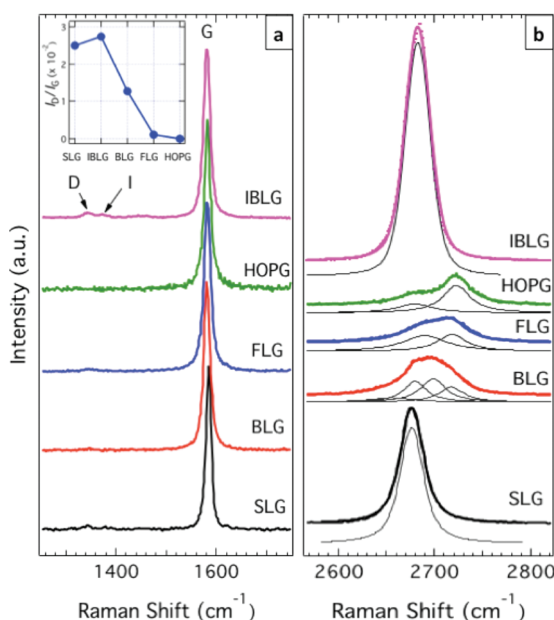


Figure 1. Raman spectra in the D and G band region (a), and the second order G' band region from single and multiple layer graphene samples (b). The inset in part a shows the I_D/I_G ratios for the various samples. All spectra are normalized with respect to the G band intensity and offset for clarity.

the region between 1650 and 2300 cm^{-1} . (1) We observe a previously unidentified dispersive mode at $\sim 1880 \text{ cm}^{-1}$ (iTA $^+$) when excited with $E_{\text{laser}} = 2.33 \text{ eV}$ in SLG, which strongly depends on the number and stacking order of graphene layers. This mode is tentatively assigned as a combination of the out-of-plane transverse optical and longitudinal optical (oTO + LO) phonons mode around the K point in the graphene Brillouin zone. (2) Another previously unidentified mode is observed at $\sim 2220 \text{ cm}^{-1}$ in SLG (when excited with $E_{\text{laser}} = 2.33 \text{ eV}$). This mode has a negative dispersion with respect to laser energy and is tentatively assigned as a combination of the iTOT and iTA phonons (iTOTA mode) around the K point. (3) The combination modes involving the LO phonon (iTA $^-$, iTA $^+$, and LOLA modes) upshift in frequency with increase in the number of graphene layers, while the iTOTA mode frequency downshifts with increasing graphene layers. An additional stiffening of all the combination modes is observed for IBLG.

RESULTS AND DISCUSSION

Figure 1a shows the D and G band region and the G' band regions from the graphene samples collected using $E_{\text{laser}} = 2.33 \text{ eV}$. Also included in Figure 1 are spectra collected from bulk graphite (HOPG). The D band intensity is very low across all graphene samples and is negligible for HOPG. Not surprisingly, the I_D/I_G value for IBLG is the highest and it decreases in general as the number of layers increase as shown in the inset in Figure 1a. In addition, a second peak in the D band region can be observed in the IBLG spectrum. This

peak, called the I band, appears at 1374 cm^{-1} and can be used as a metric for identification of IBLG (see Figure S1 in the Supporting Information for a magnified view of the I band). The 2D band from SLG, BLG, FLG, and HOPG can be fit to 1, 4, 2, and 2 Lorentzian peaks, respectively, thus confirming the presence of 1, 2, few layer graphene and bulk graphite (Figure 1b). The Raman signature from IBLG is different from both SLG and BLG, where the 2D band intensity is higher than the G band, but reverts to a single Lorentzian peak similar to SLG with a blue-shifted ($\sim 7 \text{ cm}^{-1}$) frequency.^{6,15}

Figure 2a shows peaks in the region between the G and G' bands ($1650\text{--}2300 \text{ cm}^{-1}$), which are typically much lower in intensity compared to the other peaks in the Raman spectra of graphene. The strong dependence of peak frequencies and intensities of these modes on the number of layers can be observed clearly in Figure 2a. The lowest frequency peak in Figure 2a appearing at $\sim 1750 \text{ cm}^{-1}$ is a double peak feature called the M band, which is an overtone of the oTO phonon and has been observed in graphite and single-walled nanotube (SWNT) samples.^{16,17} The M band, which is activated by strong coupling between graphene layers, is suppressed for SLG and IBLG as observed previously.¹⁴ In addition, the lower frequency peak in the M band (M^-) is downshifted by $\sim 20 \text{ cm}^{-1}$ in BLG compared to FLG or HOPG (vertical dashed line in Figure 2a). The peak at $\sim 1860 \text{ cm}^{-1}$ in SLG has been assigned to a combination of the iTA phonon and the LO phonon and can be called the iTA $^-$ mode.^{14,16} However, instead of a single peak as reported in previous studies,^{14,16} we observe a two-peak structure for this mode. Furthermore, the intensity of both peaks clearly decreases with increasing layers in graphene. We also observe these peaks in SLG samples on other substrates such as mica and quartz, confirming that the peaks are intrinsic to graphene and not a substrate effect. The third set of peaks in the range shown in Figure 2a occur due to combinations between the iTO + LA (lower frequency peak) and LO + LA phonons (higher frequency peak).¹⁴ It has recently been shown that the higher frequency LOLA peak is more sensitive to defects and decreases in intensity upon heat treatment.^{18,19} Finally a previously unidentified peak at $\sim 2220 \text{ cm}^{-1}$ is observed in all graphene samples and its origin is discussed below.

Two novel features can be observed from Figure 2a. A new mode appears at $\sim 1880 \text{ cm}^{-1}$ (iTA $^+$) as a shoulder on the higher frequency side of the iTA $^-$ peak in SLG. In addition, this new mode is greatly suppressed in IBLG in contrast with SLG and BLG, indicating that it is very sensitive to the stacking order of graphene layers. As such, we refer to the absence of this mode as an indicator for IBLG. We tentatively assign this peak to a combination of the oTO and LO phonons around the K point of the graphene Brillouin zone, as explained below. The second new feature in

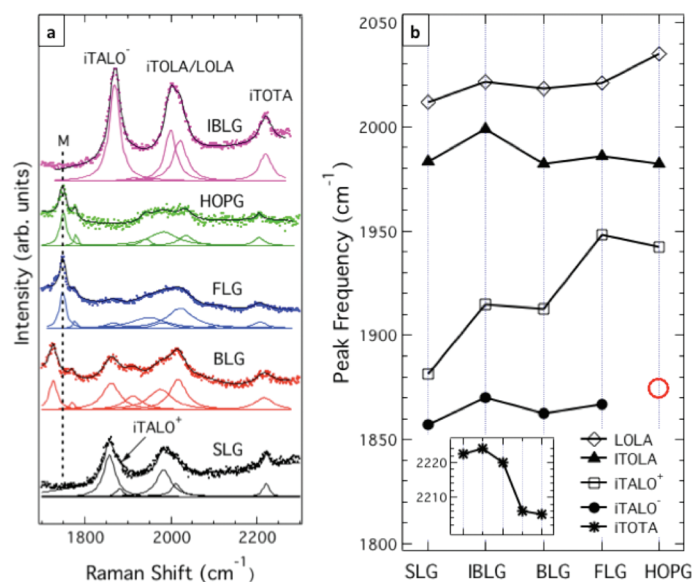


Figure 2. (a) Raman spectra between 1650 and 2300 cm^{-1} from graphene samples collected with $E_{\text{laser}} = 2.33$ eV. All spectra have been normalized by the G band intensity and fitted with Lorentzian peaks. (b) Change in peak frequency of the various second order double resonance Raman modes (see legend and main text for discussion of all the peak assignments) due to increasing layers in graphene samples. The absence of the iTALO peak at ~ 1860 cm^{-1} in HOPG is indicated by the open (red) circle. Inset in part b: Position of the iTOTA peak for the various samples. The x-axis is the same as in part b.

Figure 2a is the appearance of a peak at ~ 2220 cm^{-1} that has not been seen previously in graphene samples. This peak has, however, been observed in single-walled carbon nanotubes (SWNTs)²⁰ and is tentatively assigned as a combination of the iTA and iTO phonons around the K point in the graphene Brillouin zone.

Figure 2b plots the frequencies of all the combination modes between 1650 and 2300 cm^{-1} (iTALO⁻, iTALO⁺, iTOLA, LOLA, and iTOTA modes) for graphene samples with increasing layers. The iTALO⁻ mode is absent for HOPG. The peaks involving the LO phonon, namely the iTALO⁻ and LOLA peaks, increase in frequency due to increasing layers, while the iTOLA peak at ~ 1970 cm^{-1} remains more or less at the same position. The iTALO⁺ peak is also observed to increase in frequency, suggesting that it occurs due to the involvement of the LO phonon, analogous to the iTALO⁻ and LOLA modes. In addition, the frequency of the iTOTA mode at ~ 2220 cm^{-1} (inset in Figure 2b) is observed to decrease with increasing graphene layers. The frequency increases of the iTALO⁻, iTALO⁺, and LOLA modes indicate a high degree of sensitivity of these modes to the stacking order of graphene layers. All the combination modes in IBLG are further upshifted in frequency compared to both SLG and BLG. While multiple mechanisms may be involved in the added frequency upshift observed in IBLG, the possibility of compressive strain (or change in restoration force for the phonon vibrations) is higher for incommensurately stacked graphene layers as opposed to AB-stacked graphene. Hence, the upshift may occur due to added stiffening of the vibrational modes. We

confirmed that the relative shift of all the combination modes is maintained between the unfolded SLG and IBLG regions on the same sample, suggesting that the results shown in Figure 2b are not due to variations in electronic doping of different samples.

Interestingly, we find that all the combination mode frequencies exhibit an almost linear dependence on $1/n$ according to the following relationship: $\omega(n) = \omega(\infty) + \beta/n$, where n is the number of graphene layers, and β is a constant (Figure 3). Such a linear dependence on $1/n$ has been observed previously for the G band phonons in exfoliated graphene.¹⁰ As seen in Figure 3, the values of β for the iTALO⁻ (~ 13 cm^{-1}) and LOLA (~ 21 cm^{-1}) are comparable to shifts caused by the van der Waals interactions (~ 12 – 13 cm^{-1}) in the radial breathing modes of bundled SWNTs,²¹ indicating that the upshifts of these modes are due to van der Waals interactions caused by layer stacking rather than changes in the electronic band structure. On the other hand, the high β value for the iTALO⁺ mode (~ 68 cm^{-1}), which occurs due to a higher frequency shift with increasing graphene layers, suggests that this mode may be more sensitive to the electronic structure of graphene, similar to the 2D band.

The dispersion of the combination modes discussed above versus laser energy is shown in Figure 4. The iTOLA and LOLA modes upshift with laser energy by 204 and 223 cm^{-1}/eV , respectively. These dispersions are similar to the peak dispersions of the iTOLA and LOLA modes in graphite and SWNTs.^{17,19,22} In addition, the dispersion of the iTALO⁻ mode is ~ 140 cm^{-1}/eV , similar to the value reported recently by Cong *et al.*,¹⁴ while the dispersion of the iTALO⁺ mode is a little

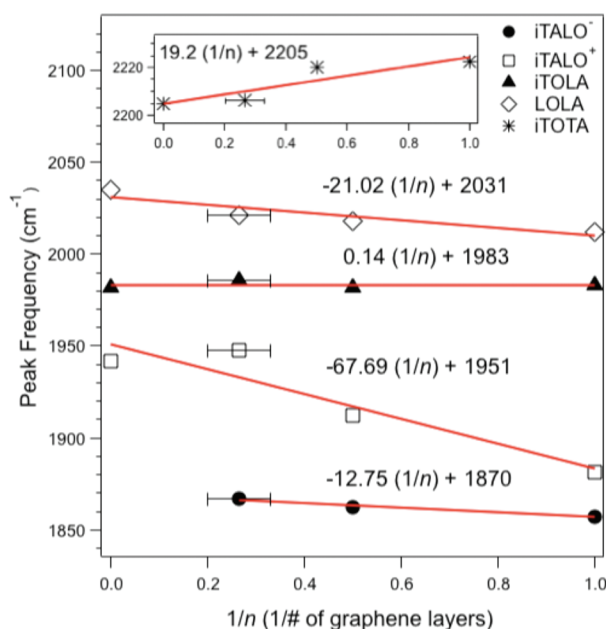


Figure 3. The peak frequencies of the $i\text{TALO}^-$, $i\text{TALO}^+$, $i\text{TALO}$, LOLA , and $i\text{TOTA}$ modes vs $1/n$. The solid lines represent the results of a least-squares fit to the data. The error bars for the FLG samples were obtained from AFM measurements which confirmed the presence of 3–5 graphene layers.

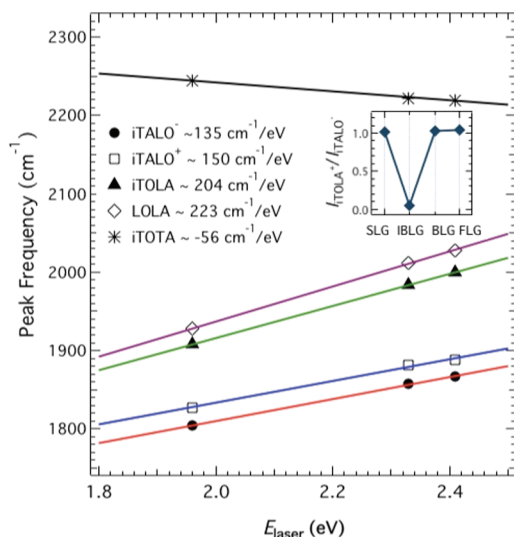


Figure 4. Dispersion of the combination modes between 1650 and 2300 cm^{-1} versus laser energy in SLG. Inset: Ratio of peak intensities of the $i\text{TALO}^+$ mode with respect to the $i\text{TALO}^-$ mode for SLG, BLG, IBLG, and FLG samples.

higher ($\sim 150 \text{ cm}^{-1}/\text{eV}$). One could consider the two peaks around 1860 cm^{-1} to occur in a similar fashion as the M band at $\sim 1750 \text{ cm}^{-1}$, which also consists of two peaks. The two-peak structure of the M band has been explained in the context of double resonance Raman scattering with the lower frequency (M^-) peak attributed to scattering by a phonon with a momentum double that of the scattered electron ($q \approx 2k$), and the higher frequency (M^+) peak due to scattering by a phonon with near-zero momentum ($q \approx 0$).¹⁷ This explains the fact that the M^+ peak does not disperse

with laser energy while the M^- peak downshifts with increasing laser energy. However, both the $i\text{TALO}^-$ and $i\text{TALO}^+$ modes are observed to shift with laser energy with similar dispersions, ruling out the $q \approx 0$ phonon within the framework of double resonance theory. Furthermore, the relative intensity between the $i\text{TALO}^-$ and $i\text{TALO}^+$ modes changes dramatically for IBLG. The inset in Figure 4 shows the ratio of peak intensities of the $i\text{TALO}^+$ and $i\text{TALO}^-$ ($I_{i\text{TALO}^+}/I_{i\text{TALO}^-}$) modes plotted for SLG, IBLG, BLG, and FLG. An obvious decrease in the ratio for IBLG can be observed, suggesting that the $i\text{TALO}^+$ peak is quite sensitive to the interlayer interaction of individual graphene layers.

A recent theoretical study predicted the absence of infrared modes in non-AB-stacked graphene.²³ The suppression of the $i\text{TALO}^+$ mode in IBLG could therefore occur due to the involvement of the infrared active oTO phonon. In addition, the $i\text{TALO}^+$ mode is observed to upshift with increasing graphene layers in a similar fashion as the $i\text{TALO}^-$ and LOLA modes (Figure 2b), suggesting that the LO phonon could be responsible for the $i\text{TALO}^+$ mode. In fact, for the $i\text{TALO}^+$ peak in HOPG at $\sim 1940 \text{ cm}^{-1}$ (see Figure 2b), a good agreement can be found for a combination of the oTO ($\sim 620 \text{ cm}^{-1}$) and LO phonon ($\sim 1350 \text{ cm}^{-1}$) around the K point of the graphene Brillouin zone.⁸ Moreover, for the excitation ranges used in this study, the dispersions of the oTO and LO phonons around the K point are both positive and could account for the $\sim 150 \text{ cm}^{-1}/\text{eV}$ dispersion of the $i\text{TALO}^+$ mode. On the basis of the above arguments we tentatively assign the $i\text{TALO}^+$ mode as a combination of the oTO and LO phonons around the K point of the graphene Brillouin

TABLE 1. Peak Frequencies and Assigned Labels for Experimentally Observed Double Resonance Raman Modes and the Peak Dispersions versus Laser Energies for Various Combination Modes in SLG and HOPG

peak freq (cm^{-1}) SLG (HOPG)	mode	phonons	dispersion (cm^{-1}/eV)	exptl observation
(1725)	M	2oTO	0	refs 16, 17
(1750)	M	2oTO	~ -10	refs 16, 17
1857	iTALO ⁻	iTA + LO	~ 135	this work and ref 14
1880 (1940)	iTALO ⁺	oTO + LO	~ 150	this work
1983 (1982)	iTOLA	LA + iTO	~ 204	refs 16, 18, 19, 22
2012 (2035)	LOLA	LA + LO	~ 223	refs 16, 18, 19, 22
2222 (2206)	iTOTA	iTA + iTO	~ -56	this work

zone. It is worth mentioning that second order modes with large dispersions (such as the iTOLA and LOLA modes) typically occur due to the combination of an acoustic and optical phonon, yet these other modes do not fit our data. Further theoretical and experimental studies are needed to understand why this particular combination mode appears for single layer and AB-stacked graphene but not IBLG.

The second previously unidentified mode in SLG at $\sim 2220 \text{ cm}^{-1}$ (for $E_{\text{laser}} = 2.33 \text{ eV}$) has a negative dispersion with laser energy and the peak frequency downshifts with increasing excitation energy by $\sim -56 \text{ cm}^{-1}/\text{eV}$ (Figure 4). A peak at $\sim 2200 \text{ cm}^{-1}$ has been observed in SWNTs but was left unassigned.²⁰ Moreover, as shown in Figure 2b, the peak at $\sim 2200 \text{ cm}^{-1}$ downshifts in frequency with increasing graphene layers in contrast to the other modes involving the LO phonon. The iTA branch around the K point has a negative dispersion and peaks around 1100 cm^{-1} corresponding to the iTA phonon have been observed in graphite whiskers¹⁶ and carbon nanotubes.²⁴ However, the dispersion of the iTA branch is ~ -75 to $100 \text{ cm}^{-1}/\text{eV}$,²⁵ which implies that the dispersion of its overtone would be twice as much. This makes it unlikely for the 2220 cm^{-1} peak to be the overtone of the iTA phonon. On the other hand, a combination of the iTA phonon (at $\sim 940 \text{ cm}^{-1}$) and iTO phonon ($\sim 1350 \text{ cm}^{-1}$) around the K point could account for the 2200 cm^{-1} mode. The iTO phonon branch has a positive dispersion ($\sim 50 \text{ cm}^{-1}/\text{eV}$) while the iTA branch has slight negative dispersion ($\sim -20 \text{ cm}^{-1}/\text{eV}$) around the K point of the graphene Brillouin zone.⁸ However, there is limited experimental data available for the iTA phonon branch around the K point of graphene (or graphite)⁸ and this ambiguity could account for the $-56 \text{ cm}^{-1}/\text{eV}$ dispersion observed for the

2220 cm^{-1} combination mode. We thus assign this mode as a combination of the iTA and iTO phonon (hence the name iTOTA) around the K point of the graphene Brillouin zone. All the combination modes discussed above are listed for SLG and HOPG in Table 1. Also included in Table 1 are the phonon modes involved in the double resonance Raman scattering process for these combination modes.

CONCLUSIONS

In summary, we have observed changes in various combination modes in the Raman spectra of graphene that depend on the number and stacking of layers. The overtone of the infrared active oTO phonon, also called the M band, disappears for SLG and non-AB-stacked bilayer samples, indicating that the M band is strongly dependent on stacking order of graphene layers. In addition, the lower frequency peak within the M band (M⁻ peak) downshifts by $\sim 20 \text{ cm}^{-1}$ for BLG compared to FLG and HOPG. A peak at $\sim 1860 \text{ cm}^{-1}$ is attributed to iTA + LO phonons, and its intensity is observed to decrease with increasing graphene layers. Moreover, the iTALO band can be deconvoluted into two peaks, with similar dispersions versus laser energy. The higher frequency peak at $\sim 1880 \text{ cm}^{-1}$ has a similar dispersion as the iTALO band and shows a strong dependence on the stacking order of graphene layers. This peak is assigned to a combination of the oTO and LO phonons around the K point in the graphene Brillouin zone. A peak at $\sim 2200 \text{ cm}^{-1}$ is observed for all graphene samples and is assigned to a combination of the iTA and iTO phonons around the K point. The peak frequencies of all the combination modes involving the LO phonon are observed to increase linearly with increasing graphene layers, indicating a strong coupling of the LO phonon between graphene layers.

METHODS

The graphene samples having various layers were prepared by using the standard mechanical exfoliation method from HOPG on 280 nm SiO₂/Si substrates (see Figures S2 and S3 in the Supporting Information for optical microscope images of the samples).²⁶ The presence of SLG, IBLG, BLG, and few layer

graphene (FLG) areas were confirmed by atomic force microscopy (AFM) and micro-Raman spectroscopy. Raman spectra were acquired with a Renishaw InVia Raman microscope using $E_{\text{laser}} = 1.96, 2.33, \text{ and } 2.41 \text{ eV}$. The incident laser beam was focused by a 50 \times objective and the laser power on the samples was kept to a minimum to avoid heating. All the Raman spectra

were normalized with respect to the G band intensity and were baseline corrected prior to Lorentzian line shape analysis.

Acknowledgment. R.R. gratefully acknowledges funding from AFOSR and the National Research Council associateship program. The material provided by R.T., J.K., D.T., and M.I. is based upon work supported by the National Science Foundation under Grant No. DMR-0955625. M.I. was supported by the summer faculty fellowship program from the American Society for Engineering Education for Summer 2010. R.P. and A.M.R. greatly acknowledge the support from COMSET and the U.S. AFOSR (No. FA9550-09-1-0384).

Supporting Information Available: Raman spectra in the D band region from IBLG and SLG showing the I band at 1374 cm^{-1} in IBLG and optical microscope images ($50\times$ magnification) of the SLG, BLG, FLG, and IBLG samples used in this study. This material is available free of charge via the Internet at <http://pubs.acs.org>.

REFERENCES AND NOTES

- Geim, A. K.; Novoselov, K. S. The rise of graphene. *Nat. Mater.* **2007**, *6*, 183–191.
- Geim, A. K. Graphene: Status and Prospects. *Science* **2009**, *324*, 1530–1534.
- Novoselov, K. S.; Geim, A. K.; Morozov, S. V.; Jiang, D.; Katsnelson, M. I.; Grigorieva, I. V.; Dubonos, S. V.; Firsov, A. A. Two-dimensional gas of massless Dirac fermions in graphene. *Nature* **2005**, *438*, 197–200.
- Zhang, Y.; Tang, T.-T.; Girit, C.; Hao, Z.; Martin, M. C.; Zettl, A.; Crommie, M. F.; Shen, Y. R.; Wang, F. Direct observation of a widely tunable bandgap in bilayer graphene. *Nature* **2009**, *459*, 820–823.
- Latil, S.; Meunier, V.; Henrard, L. Massless fermions in multilayer graphitic systems with misoriented layers: *Ab initio* calculations and experimental fingerprints. *Phys. Rev. B* **2007**, *76*, 201402.
- Ni, Z.; Wang, Y.; Yu, T.; You, Y.; Shen, Z. Reduction of Fermi velocity in folded graphene observed by resonance Raman spectroscopy. *Phys. Rev. B* **2008**, *77*, 235403.
- Ferrari, A. C.; Meyer, J. C.; Scardaci, V.; Casiraghi, C.; Lazzeri, M.; Mauri, F.; Piscanec, S.; Jiang, D.; Novoselov, K. S.; Roth, S.; Geim, A. K. The Raman Fingerprint of Graphene. *Phys. Rev. Lett.* **2006**, *97*, 187401.
- Saito, R.; Jorio, A.; Souza Filho, A.; Dresselhaus, G.; Dresselhaus, M.; Pimenta, M. Probing Phonon Dispersion Relations of Graphite by Double Resonance Raman Scattering. *Phys. Rev. Lett.* **2001**, *88*, 027401.
- Ferrari, A. C.; Meyer, J. C.; Scardaci, V.; Casiraghi, C.; Lazzeri, M.; Mauri, F.; Piscanec, S.; Jiang, D.; Novoselov, K. S.; Roth, S.; Geim, A. K. Raman Spectrum of Graphene and Graphene Layers. *Phys. Rev. Lett.* **2006**, *97*, 187401.
- Gupta, A.; Chen, G.; Joshi, P.; Tadigadapa, S.; Eklund, P. Raman scattering from high-frequency phonons in supported n-graphene layer films. *Nano Lett.* **2006**, *6*, 2667–2673.
- Cançado, L.; Reina, A.; Kong, J.; Dresselhaus, M. Geometrical approach for the study of G' band in the Raman spectrum of monolayer graphene, bilayer graphene, and bulk graphite. *Phys. Rev. B* **2008**, *77*, 245408.
- Malard, L.; Pimenta, M.; Dresselhaus, G.; Dresselhaus, M. Raman spectroscopy in graphene. *Phys. Rep.* **2009**, *473*, 51–87.
- Gupta, A. K.; Tang, Y.; Crespi, V. H.; Eklund, P. C. A non-dispersive Raman D-band activated by well-ordered interlayer interactions in rotationally stacked bi-layer Graphene. *Phys. Rev. B* **2010**, *82*, 241406.
- Cong, C.; Yu, T.; Saito, R., Second-order Overtone and Combinational Raman Modes of Graphene Layers in the Range of 1690 cm^{-1} to 2150 cm^{-1} . **2010**, arXiv:1010.3391v1.
- Poncharal, P.; Ayari, A.; Michel, T.; Sauvajol, J. L. Raman spectra of misoriented bilayer graphene. *Phys. Rev. B* **2008**, *78*, 113407.
- Tan, P.; Dimovski, S.; Gogotsi, Y. Raman scattering of non-planar graphite: arched edges, polyhedral crystals, whiskers and cones. *Philos. Trans. R. Soc., Ser. A* **2004**, *362*, 2289.
- Brar, V.; Samsonidze, G.; Dresselhaus, M.; Dresselhaus, G.; Saito, R.; Swan, A.; Unlü, M.; Goldberg, B.; Souza Filho, A.; Jorio, A. Second-order harmonic and combination modes in graphite, single-wall carbon nanotube bundles, and isolated single-wall carbon nanotubes. *Phys. Rev. B* **2002**, *66*, 155418.
- Ellis, A. Second-order overtone and combination modes in the LOLA region of acid treated double-walled carbon nanotubes. *J. Chem. Phys.* **2006**, *125*, 121103.
- Rao, R.; Reppert, J.; Zhang, X. F.; Podila, R.; Rao, A. M.; Talapatra, S.; Maruyama, B., Double resonance Raman study of disorder in CVD-grown single-walled carbon nanotubes. *Carbon*. DOI: 10.1016/j.carbon.2010.11.052. Published Online: Dec 2, 2010.
- Tan, P.; Tang, Y.; Deng, Y. M.; Li, F.; Wei, Y. L.; Cheng, H. M. Resonantly enhanced Raman scattering and high-order Raman spectra of single-walled carbon nanotubes. *Appl. Phys. Lett.* **1999**, *75*, 1524.
- Rao, A. M.; Chen, J.; Richter, E.; Schlecht, U.; Eklund, P. C.; Haddon, R. C.; Venkateswaran, U. D.; Kwon, Y. K.; Tománek, D. Effect of van der Waals Interactions on the Raman Modes in Single Walled Carbon Nanotubes. *Phys. Rev. Lett.* **2001**, *86*, 3895.
- Fantini, C.; Pimenta, M.; Strano, M. Two-Phonon Combination Raman Modes in Covalently Functionalized Single-Wall Carbon Nanotubes. *J. Phys. Chem. C* **2008**, *112*, 13150–13155.
- Jiang, J.-W.; Tang, H.; Wang, B.-S. Raman and Infra-red properties and layer dependence of the phonon dispersions in multi-layered graphene. *Phys. Rev. B* **2007**, *77*, 23.
- Dresselhaus, M.; Eklund, P. Phonons in carbon nanotubes. *Adv. Phys.* **2000**, *49*, 705–814.
- Saito, R.; Jorio, A.; Souza Filho, A. G.; Grueneis, A.; Pimenta, M. A.; Dresselhaus, G.; Dresselhaus, M. S. Dispersive Raman spectra observed in graphite and single wall carbon nanotubes. *Phys. B (Amsterdam, Neth.)* **2002**, *323*, 100.
- Novoselov, K. S.; Jiang, D.; Schedin, F.; Booth, T. J.; Khotkevich, V. V.; Morozov, S. V.; Geim, A. K. Two-dimensional atomic crystals. *Proc. Natl. Acad. Sci. U.S.A.* **2005**, *102*, 10451–3.